Modeling of Moisture Transport in Wood with Hysteresis and Temperature-Dependent Sorption Characteristics

Carsten Rode, Ph.D. **Christian Odin Clorius, Ph.D.**

ABSTRACT

Transient calculation models that predict moisture content in wood and other hygroscopic construction members employ the sorption curve of the materials to express the relationship between relative humidity of air and equilibrium moisture content. However, the sorption curves are somewhat temperature dependent, and they exhibit hysteresis, so the equilibrium state depends on the sorption history. Most transient moisture transport models neglect these facts. This paper will attempt to refine the current models by implementing a sorption "surface" spanned by relative humidity, temperature, and the resulting moisture content.

The paper mainly indicates that taking hysteresis into account will tend to reduce the effective moisture capacity of building materials for short-term moisture variations, while taking the influence of temperature on the sorption properties into account will tend to increase the apparent moisture capacity in practical situations where heating of a building element is normally ensued by its drying.

The paper will investigate the effect of considering moisture content dependency of the vapor permeability, sorption hysteresis, and temperature dependency of the sorption curves in an existing calculation model, which is used to predict the moisture conditions in solid wood constructions. This paper presents measurements of moisture content in almost 5-in.-thick roof elements of solid wood, which are located over an open stable for cattle. A previous comparison between measurement and prediction of the moisture content of the wood had indicated the possibility of using temperature-dependent sorption data as a way to improve the correspondence—particularly the question about the magnitude of the seasonal variations. The calculation results with the new model are presented alongside with experimental results and practical experiences of such constructions.

INTRODUCTION

The influence of moisture content on the mechanical behavior of timber constructions is traditionally and according to the European code (Eurocode 5 2001) handled by the system of service classes and the corresponding modification factors. Whereas this system is very expedient and rational with respect to the strength and stiffness properties, there is a shortcoming of the system regarding the assessment of fluctuations of moisture content within the service classes. This assessment is needed both in the case where changes in moisture content give rise to global deformations of the structure (for an example, see Clorius [2003]) and in cases where moisture-induced deformations give rise to internal stresses and, hence, formally should be treated as a load case.

The present investigation is a refinement to present tools for numerical assessment of moisture fluctuations in wood as it presents an implementation of a procedure for determining moisture transport and moisture content by use of temperature-dependent sorption characteristics. This is particularly relevant for wood members at outdoor covered conditions. The procedure is implemented as an extension to an existing computer model (Pedersen 1990a) for moisture and temperature calculations for constructions of hygroscopic materials.

The background ideas for engaging in the present investigation arose in consequence of the following two observa-

Carsten Rode is an associate professor and **Christian Odin Clorius** is an assistant professor in the Department of Civil Engineering, Technical University of Denmark, Lyngby, Denmark.

tions made when using the existing tools for determining wood moisture content in response to natural climate variations:

- Wood members exposed to variations in the ambient climate air temperature, T_{air}, and relative humidity, RH, show a damped transient moisture content response. The magnitude of the damping depends on the value of the permeability and member thickness. For thick wood members, the variation of the transient moisture content is significantly smaller than the variation of equilibrium moisture content governed by the climate variations.
- Wood members exposed to repeated variations in the ambient climate have mean moisture content, which is higher than the equilibrium moisture content determined, assuming mean value of the ambient climate conditions. The elevated moisture content is due to the water vapor permeability of wood increasing significantly with the moisture content. The wooden member is more permeable and open to moisture uptake at high values of ambient RH than it is at low values of ambient RH. Consequently, thick wood members are provided with a "moisture-trap" function elevating the mean moisture content.

The damped response in moisture content (MC) of thick members is generally known. In practice, however, it is often only tentatively quantified, and structural engineers tend to overestimate the amplitude of the MC fluctuations. The effect of the shape of the water vapor permeability function, δ_p(RH), on the long-term mean transient moisture content of wood has been identified in Arfvidsson (1999) and in Clorius and Pedersen (2003). The effect is not generally recognized, but modeling shows that the effect is not negligible for thick wood members in the Nordic climates.

The modeled long-term mean transient moisture content for thick wood members at outdoor covered conditions, such as presented by Clorius and Pedersen (2003), exhibits small amplitude in annual MC variation. For recurring exposure to a Danish climate, the modeled amplitude is in the order of less than 1% moisture content by weight. This variation is suspiciously small, and by any means in the same order as the variation of the sorption characteristic with temperature. Hence, the inclusion of a temperature-dependent sorption characteristic might increase the modeled long-term annual MC amplitude. This paper addresses the implementation of such temperature-dependent sorption characteristics and tentatively tests modeling results against field measurements made in a solid wood roof construction over a two-year period. Furthermore, the paper presents a study of the effect of including and, respectively, not including hysteresis in combination with temperature-dependent sorption characteristic.

MODELING METHOD

Karagiozis (2001) reports on a hygrothermal simulation model that includes temperature dependency of the sorption curves and mentions that this feature is important when simulating wood-based material elements. However, no results of this importance seem to be reported in literature. One should also observe the fact that, even if such functionality were present, the practical problem of obtaining reliable experimental sorption data at temperatures other than 20°C (68°F) remains. However, this paper will present the development and use of a model that takes the temperature effect into account. The model will be used to analyze a case of a wood-based structure, and wood is a material for which temperature-dependent sorption data can be found in the literature.

The modeling of moisture content has been performed by use of an existing computer model for transient calculation of combined heat and moisture transport (Pedersen 1990a), which has been modified to take into account the temperature dependency of the sorption curves of materials. In the present context, the model has the following functionalities:

- Sorption-isotherm can be defined with an adsorption and desorption branch.
- Hysteresis can be modeled in an empirical way (Pedersen 1990b).
- A moisture-dependent water vapor permeability can be defined.
- The model is capable of calculating several moisture transport forms (e.g., vapor, liquid, and convective).
- The load history can be defined in time series for temperature and relative humidity, covering periods of a year or more with data points in one-hour intervals.

Material data, such as the water vapor permeability or data for the sorption curves, are entered in the program's database as a list of data points that describe each parameter's dependency on other parameters. For instance, a sorption curve is described as a number of points of type (RH-MC), and the program makes linear interpolation between them. With this approach, more accuracy can be achieved by increasing the number of data points, and it has the advantage that original measuring points can be used directly as input for the program. Furthermore, it is not dependent on a predefined functional form of the data and, therefore, does not rely on how well the functional form fits the actual material data.

The model employed is based on finite control volumes and uses an implicit scheme for the numerical solution of the finite difference equations. However, since the material properties are not constant, the problem is nonlinear, and a certain procedure needs to be followed to ensure good approximation of the moisture-dependent variables, conservation of mass of the overall solution, and speed of calculation:

- The temperature distribution is calculated first in each time step. The temperatures are found in a transient way

also using a finite control volume approach and considering solar gain on the external surface, longwave radiation to the sky, moisture-dependent thermal conductivities, and latent heat of phase change of moisture. The temperature distribution determines the new distribution of saturation vapor pressures.

- The finite difference equations are set up based on a formulation that uses vapor pressure, p, as the determining variable. Vapor pressure is the driving force for vapor diffusion according to Fick's law, and via the slope of the sorption curve, ξ, and knowledge of the saturation vapor pressures, p_s, in the beginning and end of the time step, the change of moisture content, u, of each control volume can be expressed by changes in relative humidity, p/p_s. Liquid transport is considered as an explicit source term found from Darcy's law using the liquid pressures, P_l, from the previous time step. In differential form, the equation can be set up as

$$\rho\xi(\varphi)\frac{\partial\left(\frac{p}{p_s}\right)}{\partial t} = \frac{\partial\left(\delta(\varphi)\frac{\partial p^{new}}{\partial x}\right)}{\partial x} + \frac{\partial\left(K(u)\frac{\partial P_l^{old}}{\partial x}\right)}{\partial x}. \qquad (1)$$

The material properties needed are the density, ρ, water vapor permeability, δ, and the slope of the sorption curve, and they are found from the last known relative humidity, φ. Also used is the liquid water permeability, K, which is found at the last known moisture content. A new vapor pressure distribution is found for the whole calculation domain by solving the set of equations (Equation 1) for all control volumes.

- A similar procedure is used to determine new liquid pressures based on suction curves that give the relationship between change of moisture content and change of liquid pressure. The slope of the suction curve is $\Xi = \partial u / \partial P_l$. Vapor diffusion is calculated as an explicit source term based on the vapor pressures from the previous time step.

$$\rho\Xi(u)\frac{\partial(P_l)}{\partial t} = \frac{\partial\left(\delta(\varphi)\frac{\partial p^{old}}{\partial x}\right)}{\partial x} + \frac{\partial\left(K(u)\frac{\partial P_l^{new}}{\partial x}\right)}{\partial x} \qquad (2)$$

New liquid pressures are found by solving the set of equations (Equation 2) expressed in liquid pressure.

- The new moisture contents are determined from a continuity equation determining the increment in moisture content from Fick's and Darcy's laws using the new vapor and liquid pressures.

$$\rho\frac{\partial u}{\partial t} = -\frac{\partial g_v}{\partial x} - \frac{\partial g_l}{\partial x} \qquad (3)$$

where ∂g_v and ∂g_l are water vapor and liquid fluxes, respectively.

The new relative humidity is found from the new moisture content and the sorption curve.

- The model also has provisions for calculating moisture transport by convection in the form of moisture carried with infiltrating air. This feature will not be used in this paper.

Hysteresis

The program code handles scanning curves by an empirical approach using the weighted values of the slope of the adsorption and desorption branch.

$$\xi_a = \frac{\partial u_a}{\partial\varphi} \quad \text{and} \quad \xi_d = \frac{\partial u_d}{\partial\varphi} \qquad (4)$$

where ξ_a and ξ_d are slopes of the sorption curves, or "specific moisture capacities," for the adsorption and desorption curves, respectively.

When the most recent moisture history—the two preceding time steps—shows an increase in MC, the slope of the adsorption scanning is determined by

$$\xi_{hys,a} = \frac{0.1(u-u_a)^2\xi_d + (u-u_d)^2\xi_a}{(u_d-u_a)^2}, \qquad (5)$$

where u_a and u_d are the moisture contents on the adsorption and desorption curves corresponding to the current relative humidity, and u is the most recently determined moisture content. Correspondingly, the slope of the desorption scanning curve is determined by

$$\xi_{hys,d} = \frac{(u-u_a)^2\xi_d + 0.1(u-u_d)^2\xi_a}{(u_d-u_a)^2}. \qquad (6)$$

This empirical paradigm for modeling hysteresis has proven to be a well working way to improve the description of transient sorption processes in materials and is today a standard feature of the program used for this paper. The effect of the hysteresis is a reduction of the apparent moisture capacity of a material. Since the scanning curves have a lower slope than the adsorption and desorption isotherms, the effect will be a larger variation in local vapor pressure when the moisture content of a material is varying. Thus, hysteresis is worthwhile considering when the short-term dynamic moisture response of a material is of interest. It may be one of the explanations of a phenomenon such as "retarded sorption" or "non-Fickian" behavior (Håkansson 1998; Peuhkuri 2003), which is especially observed for organic-based materials. However, when the interest is the long-term behavior of a construction part in a building envelope, it may not be relevant to consider the intermediate (daily) variations that result from the scanning curves, and then the mean curve between adsorption and desorption can be used (Pedersen 1990b).

The objective of the present paper is not to explore the effect of changes to the above empirical formulation of hysteresis; indeed, some investigations (e.g., Goossens [2003])

suggest that there is still room for improvement of the coefficients of the model suggested by Equations 5 and 6. The objective of this paper is to investigate the effect of including temperature-dependent sorption given the previous choice of hysteresis formulation.

Temperature-Dependent Sorption Characteristic

The temperature dependency of the sorption characteristic is taken into account in the modeling procedure by allowing several sorption curves to describe the sorption characteristics at different temperature levels.

An arbitrary number of sorption isotherms can be used, as the model makes linear interpolation between them when it retrieves the sorption properties it needs. Thus, each time the model needs a property of the sorption curve, e.g., the relationship between moisture content and relative humidity, or the slope of the curve at a given relative humidity, then the temperature is passed as a parameter in the call for that property. The sorption characteristics of a material are represented as a body in the three-dimensional space, which is defined by axes for temperature, relative humidity, and moisture content. The body is confined between a lower surface for adsorption and an upper surface for desorption (see Figure 1).

The principle of using the temperature-dependent sorption data is relatively straightforward. The computer model is based on an implicit finite control volume method formulated with the vapor pressure as driving potential. This method uses the slope of the sorption curves as an input, and the result is the new distribution of vapor pressures. New moisture contents are found by the end of each time step as an increment from the old values, which is calculated based on Fick's law and the new vapor pressures. Before calculating the next time step, it is checked that the (RH^{new}, MC^{new}) data point is within the constraints given by the adsorption and desorption curves or, if not, the relative humidity is corrected.

It is well known, that water absorbed in porous materials experiences some depression of the freezing point depending on the pore size distributed. Wood, however, may be regarded as partially dissolved in the absorbed water (Skaar 1988), that is, as a gel where hygroscopic water is bound to the cell wall constituents (cellulose, hemicellulose, and lignin). Thus, hygroscopic water in wood ranges from nonfreezing water to water with freezing point depression depending on the strength of the binding forces. In Sellevold et al. (1975), there is indication that phase changes for hygroscopic water in wood first occur at –90°C (–130°F); hence, for all practical purposes, hygroscopic water can be regarded as nonfreezing. Even free water above the fiber saturation point has freezing point depression, both due to the effect of capillary depression and due to water-soluble extractives in the capillary water further reducing the vapor pressure. For the calculation model, it has been chosen to represent the saturation vapor pressure by its value over ice, as opposed to over supercooled water, for all temperatures below 0°C (32°F). All input data for the calculation model (weather data and sorption properties) have been prepared on this basis.

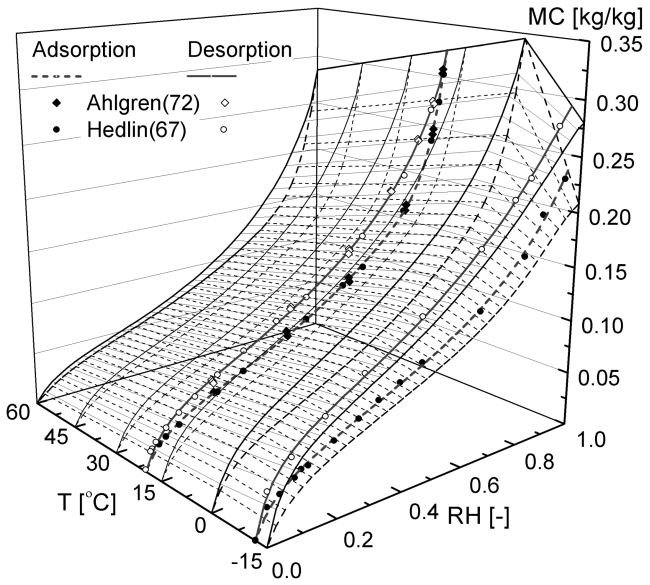

Figure 1 *Full sorption for Picea abies (Norway spruce). Note that the RH is given relative to water for T > 0°C (32°F) and relative to ice for T < 0°C (32°F); this is in accordance with the international meteorological convention. Experimental data for EMC determined in adsorption and desorption determined at 20°C (68°F) on Picea abies with a mean density of 420 kg/m^3 (26 lb/ft^3) (Ahlgren 1972) and on Picea alba at 21°C (70°F) and –12°C (10°F) (Hedlin 1967) are given.*

MOISTURE CAPACITY AND TRANSPORT PARAMETERS

Sorption Characteristic for Picea Abies

Numerous researchers have investigated the sorption characteristic for wood experimentally and theoretically (Stamm 1964; Kollmann and Côté 1968; Skaar 1988). The general shape of the isothermal sorption characteristic is well established: a double sigmoid curve with lower equilibrium moisture content (EMC) in adsorption compared to desorption; the two branches are assumed to meet and close the sorption curve at the fiber-saturation point corresponding to the maximum value for hygroscopic bound water and stipulated to be the EMC for RH→1. However, the physics behind the observed isothermal shape is disputed. Venkateswaran (1970) lists 18 sorption equations having been proposed to explain the sorption mechanism of cellulosic materials, and new approaches are still being proposed—most recently in Bingye and Avramidis (2003). Skaar (1988) groups sorption models thematically by their physical basis and treats the different model categories thoroughly.

The relation between sorption characteristics at different temperatures is widely recognized to be explainable by thermodynamics of sorption via an application of the Clausius-Clapeyron equation to the differential heat of sorption. The differential heat of sorption ΔH_S, i.e., difference in energy needed to vaporize sorbed water and free water, is assumed to be temperature independent and, at isosteric conditions, obey the following relation between temperature and activity:

$$[\Delta H_S]_{MC} \approx R \cdot T_1 \cdot T_2 [\ln(RH_2/RH_1)/(T_2 - T_1)]_{MC} \qquad (7)$$

where R is the ideal gas constant. As the differential heat of sorption is a positive quantity, a positive temperature increment $T_2 > T_1$ will entail that the isosteric MC be reached in equilibrium with a value of the relative humidity $RH_2 > RH_1$. Thus, the isobaric EMC decreases for increasing temperature. The Clausius-Clapeyron equation (Equation 7) has been implemented in numerous instances, often in a context where the integrated differential heat of sorption is determined on the basis of isosteric readings on two or more isotherms and compared to calorimetric determinations of the total heat of wetting, e.g., Strømdahl (2000). Skaar (1988) compiles many of the reported investigations in a comprehensive collection. Cudinov et al. (1978a, 1978b) use Equation 7 to argue that the maximum value of hygroscopically bound water is obtained for $T = 0$°C (32°F), and that EMC will decrease on both sides of the freezing point isotherm except for small values of EMC.

In the present context, the theoretical approaches summarized above have only been employed as overall guidelines in a more empirical approach for establishing a full sorption surface. The strategy for establishing the adsorption and desorption surfaces has been to use a slender but well-established empirical basis for isothermal sorption at different temperatures and connect these experimental evidences in the three-dimensional sorption space (T-RH-MC), thus generating the necessary data-set input for the model. In order to get full use of the available experimental data at isothermal conditions, the sorption fit model given in Equation 8 has been used. The model is a slight rewriting of a fit-model originally presented in Nielsen (1989) and used in a comparative study of sorption models in Strømdahl (2000). In the original version, the model is rationalized in the theoretical framework of the BET theory. However, in the present context, it is used not for its theoretical merits but for its ability to conform to the shape of the empirical data. Hence, the five parameters (P1 – P5) of Equation 8 are to be viewed as pure fit parameters in the procedure for nonlinear least-squares regression analysis of dimensionless RH as dependent variable to dimensionless MC as independent variable.

$$MC = \left(\frac{1 - RH^{P1}}{1 - RH} + \frac{RH^{P1 \times P2} \cdot (1 - RH^{P2 \times P3})}{1 - RH^{P2}} \right) \frac{P4 \cdot RH}{1 + P5 \cdot RH} \qquad (8)$$

The setpoint for the sorption surface has been the canonical Scandinavian values for the sorption-isotherm for *Picea abies* (Norway spruce) (Ahlgren 1972). These data, here quoted from Hansen (1986), were generated at isothermal 20°C (68°F) conditions for material with a mean density of 420 kg/m^3 (26 lb/ft^3), a density in proximity to the material used in the case study. The second set of data originates from Hedlin (1967), where the sorption isotherms for *Picea alba* at subfreezing temperature, –12°C (10°F), and at reference temperature, 21°C (70°F), are presented. It should be recognized that the subfreezing isothermal sorption tests by Hedlin (1967) are the largest subfreezing test series for cellulosic materials reported in the literature and practically the only one available for wood (see Cudinov et al. [1978a]). From a sorption point of view, *Picea alba* and *Picea abies* are expected to behave similarly, and the data from both species prove to be indiscernible at the reference temperature. Hence, it is assumed that the subfreezing values for *Picea alba* are valid also for *abies*. Both sets of experimental data are shown in Figure 1 along with fits by means of Equation 8. Observe that though the used fit model is not defined for $RH = 1$, it has a limit value that is used. At reference 20°C (68°F) conditions, the fits to adsorption and desorption based on data from Hedlin (1967) and Ahlgren (1972) jointly meet in a marginally different limit value corresponding to a fiber saturation point of 33% moisture content by weight.

At subfreezing conditions, the adsorption and desorption branches shown in Figure 1 do not meet in a common fiber saturation point. That this is correct and not due to an error on the reported data stems from the shift of basis for relative humidity at $T = 0$°C (32°F). At above-freezing temperatures, the saturation vapor pressure is determined over a plane water surface, $p_{sat,w}$, and at subfreezing temperatures, the saturation vapor pressure is determined over a plane surface of ice, $p_{sat,i}$. Shift in saturation pressure base can be expressed as $p_{sat,i} = \beta(T) p_{sat,w}$, where $\beta(T) < 1$. Hence, as hygroscopic water in wood is nonfreezing, the hygroscopic sorption capacity of the material does not reach true fiber saturation when $RH_i \rightarrow 1$. The hygroscopic sorption capacity would first be reached at $RH_w \rightarrow 1$, assuming a boundary condition corresponding to saturated vapor pressure over supercooled water. Thus, as the saturation vapor pressure relative to ice, $p_{sat,i}$, is an arbitrary choice from the point of view of hygroscopic capacity of the wood, the ice basis entails that the isotherm corresponding to base supercooled water is simply truncated at the value $\beta(T)$, and the isotherm appears open at $RH_i \rightarrow 1$. At the temperature –12°C (10°F) used in reported subfreezing tests by Hedlin (1967), the water-ice base ratio is $\beta = 0.88$.

The use of an ice basis at subfreezing temperatures is by far the most natural choice, as boundary conditions of vapor over water in a supercooled state will not appear under natural conditions. However, there is one additional remark to be made regarding the desorption branch at subfreezing temperatures: the desorption is a "first desorption" branch only reached when the domain is entered from higher temperatures. That is, sorption sites made available at a higher temperature will not be reactivated after the first desorption at a lower

subfreezing temperature. This is to be seen in analogy with the irreversible loss of sorption sites during first desorption from green state—only the subfreezing first desorption is reversible when reentering the domain again from higher temperature, but irreversibly lost at isothermal conditions. This remark entails that the sorption surface of Figure 1 should ideally be equipped with an additional desorption surface at subfreezing temperature for reversible desorption after first desorption. Data for construction of this second and later subfreezing desorption branch does not exist. Hedlin (1967) "wets" the specimens after adsorption at a higher temperature and desorps from this state. Hence, this refinement has not been implemented in the program code, and all states between the adsorption and desorption surfaces at subfreezing temperatures are allowed. Concerning the case study, the refinement is of minor importance because subfreezing temperatures in the Danish climate are reached only occasionally. However, in more northern regions with permanent subfreezing temperatures, the drying of wood during winter will be more pronounced than predicted from modeling using the sorption surfaces of Figure 1.

The Hedlin-Ahlgren setpoint data at 20°C (32°F) have been given isobaric extensions for all above-freezing temperatures, as seen in Figure 1. These extensions have been established by use of the isobar temperature-dependent slopes, α, that can be determined from the adsorption and desorption data reported by Kelsey (1956) at four equidistant isothermal conditions between 10°C (50°F) and 55°C (131°F). Though more investigations of temperature dependency of sorption above-freezing temperature exist, the data from (Kelsey 1956) are the most consistent and comprehensive. The tested material was *Araucaria klinkii* Lauterb. (Klinki pine). The isobaric temperature-dependent slopes, α, are notwithstanding applied directly to the *Picea abies* sorption surface. The compiling procedure consists of individual sorption fits by use of Equation 8 to each of the eight series of adsorption and desorption data. RH-equidistant fit-values for each of the four isothermal conditions are plotted with RH increments of 2.5% in a T-MC diagram, as shown in Figure 2. In this diagram, a linear regression procedure with temperature as an independent variable is employed to generate the isobars. The data yield gradually decreasing isobar slopes and comply to the linear regression with coefficients of determination r^2 in excess of 0.99 except for the isobars at RH > 0.875. It is observed that the Clausius-Clapeyron equation is fulfilled by isosteric readings of (RH,T)-data sets in Figure 2.

The trend in the data from Kelsey (1956) for near-fiber saturation shows an approximate 0.1% decrease in MC by weight pr. 10°C (18°F) temperature increase. This corresponds to an above-freezing trend reported by Stamm and Loughborough (1935) and others (see, e.g., Skaar [1988]). Most handbook values for temperature dependency follow the same trend, e.g., Forest Products Society (1999). The experimental results presented by Drewes (1985) confirm the observation made from Figure 2 that the slope of the temperature

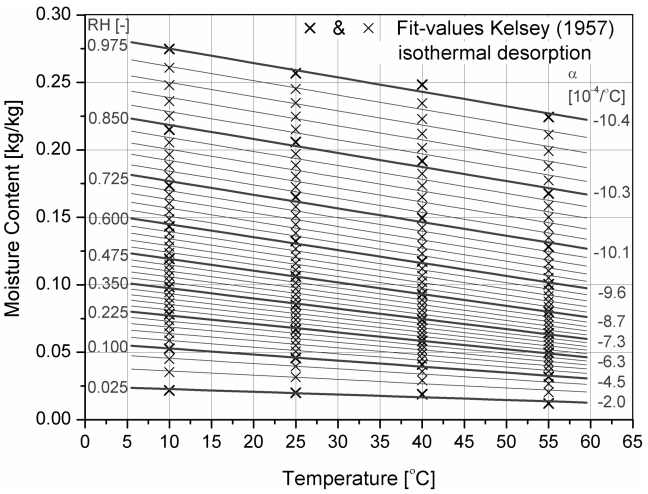

Figure 2 *Isobar diagram with indicated temperature dependency. The isobars are generated by use of isothermal desorption data from Kelsey (1956).*

dependency decreases for decreasing RH. The sorption surfaces in Figure 1 have been finalized by use of the isobar slopes of Figure 2 and a corresponding diagram generated for adsorption. The trace of the setpoint data at reference temperature in T = 0°C (32°F) is linearly connected to the Hedlin (1967) data in –12°C (10°F) and given a modest extrapolation to –15°C (5°F). The surface has not been extended beyond 60°C (140°F), as initiating plasticization of the cell wall constituents might change the sorption behavior at high temperatures (Stamm 1964) and render further linear extrapolation invalid.

Water Vapor Transport Characteristic

The water vapor characteristic for perpendicular to grain transport is determined on the basis of a regression on experimental data for *Picea abies* with mean density in the range 400-430 kg/m^3 (25-27 lb/ft^3), determined at 20-25°C (68-76°F). The data stem from cup-tests reported by Tveit (1966), Hedenblad (1996), and Fynholm and Clorius (2002); all data are shown in Figure 3. In the regression, the data from Fynholm and Clorius (2002) are given more weight, as these data are generated by use of an experimental setup, where on the order of 100 times more material is tested compared to the traditional small-size cup-test specimen. These tests were performed on glued solid wood elements similar to those of the case study construction presented in this paper.

The water vapor permeability function, δ_p(RH), as shown in Figure 3, is valid in the indicated temperature range but, in the modeling procedure, it is used as a universal transport coefficient function valid for all temperatures. This is primarily due to the lack of permeability values at other temperatures, although the data from Tveit (1966) at other temperatures shown in Figure 3 could indicate that the perme-

ability decreases with temperature. However, with a lack of further knowledge, the outlined procedure with a temperature-independent permeability characteristic is chosen.

With regard to the problems of diffusion as such, it is noted that many of the abnormalities observed and attributed to "non-Fickian" behavior can be explained if the traditional Fickian diffusion model is replaced by the "double" Fickian model established by Krabbenhøft (2003). His model operates with parallel diffusion of water vapor and diffusion of cell wall bound water and includes the velocity of sorption and its dependency of moisture increment step size and degree of saturation. This model put forward in Krabbenhøft (2003) is very convincing in its ability to model the diffusion abnormalities observed by Wadsö (1993). Within this paper, however, the diffusion model is more traditional, and the focus is primarily the effect of a temperature-dependent sorption characteristic.

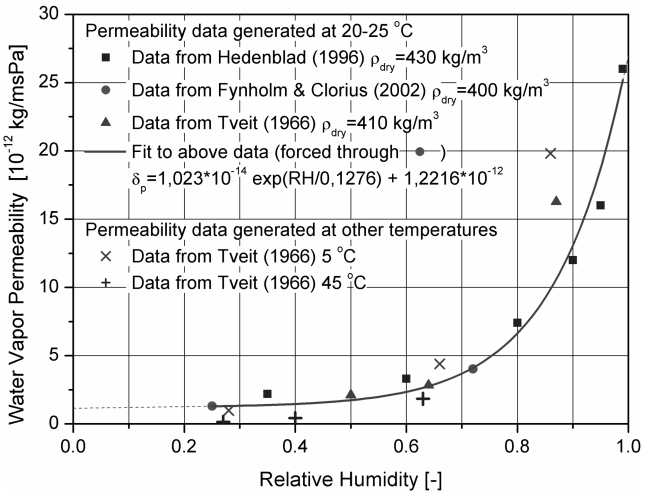

Figure 3 *Experimental data and derived water vapor characteristics as a function of relative humidity for Picea abies perpendicular to the grain.*

SOLID WOOD CASE STUDY CONSTRUCTION

Construction and Field Measuring

Measurements of wood moisture content have been made in the solid wood roofing construction of a stable at the Centre for Living Cultural Heritage at the Danish Agricultural Museum during the period of 2002-2003. The construction serves as a naturally ventilated stable with open facades and central apex skylight ventilation. The construction has portal frames covered with solid wood elements spanning in single span between the frames, establishing a roof with a slope of 22° (see Figure 4). The elements are freely exposed to the ambient climate at the lower ceiling surface and have a nailed asphalt roofing felt on top. The lamella species is *Picea abie*s, and the elements are produced as ordinary glued laminated timber with a mean density in the range 400-430 kg/m^3 (25-27 lb/ft^3). The elements are 325 mm (13 in.) wide with a thickness of 120 mm (4.8 in.); the inter-element connection is established by screws through a inserted plywood tongue as shown in Figure 4. For a more thorough description of the construction, see Clorius and Ljørring (2003).

Measurements of wood moisture content are carried out in a total of 12 positions in the solid wood elements on a west-facing roof surface. The overall position of the measuring points is along a section from the overhang to apex centrally in the construction. The points are positioned approximately 1.2 m (4 ft) from the jointed ends of the element butt over the adjacent portal frame. Relative to the element cross section, there are three types of measuring positions (Figure 4). In the present paper, only measuring results from the four lower side positions are reported. All positions measure maximum MC over a length of 25 mm (1.0 in.) in the thickness direction of the elements. The lower side positions measure from a depth of 10 mm (0.4 in.) from lower side and inward and are positioned centrally in the mid-element lamella relative to element

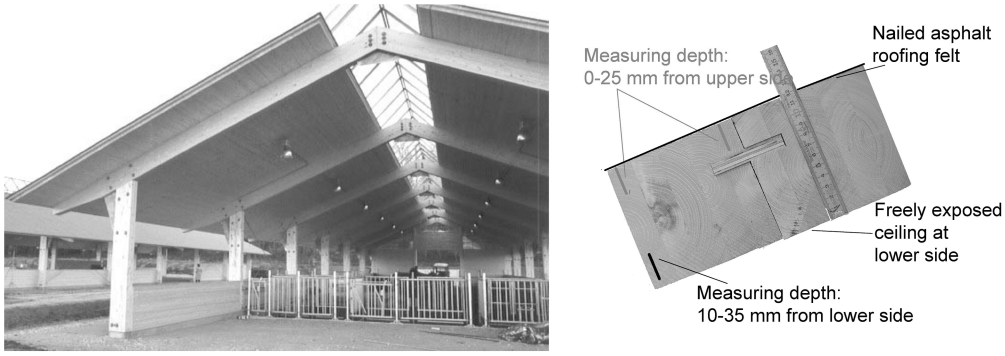

Figure 4 *View case study construction with inserted detail view of element with indication of measuring location relative to element.*

width (Figure 4). The reported measurements are intended to measure MC in a region where moisture transport is dominated by diffusion through the element in the transverse direction of the wood.

Measuring Method and Calibration Corrections

The measuring method employed is based on the traditional resistance-type moisture content meter method. The measuring system uses permanently inserted stainless-steel screws as electrodes at the measuring positions. The electrodes were inserted via 16 mm holes drilled from the element's upper side to the prescribed depth. As this procedure incurs some inaccuracy and as the electrode-screw unwillingly can have been countersunk in the insertion process, the nominal measuring depths given in Figure 4 should probably be given an uncertainty of ±5 mm. Attention is drawn to the fact that the electrodes have a finite extension in the direction of the moisture gradient (25 mm) (1.0 in.), and resistance-type measuring always gives the highest value of MC in the region between the uninsulated electrodes. Hence, the measured values are maximum MC values obtained in a region with at least 25 mm (1.0 in.) extension in the gradient direction, and the position of the maximum value is not necessarily the same throughout a season.

To avoid intrusion of water and water vapor through the insertion holes, these were carefully filled with silicone sealant after electrode insertion. The disturbance of the moisture transport field above the measuring point due to the sealant-filled hole is assessed to be of minor importance as the permeability to moisture transport velocity in the longitudinal direction is approximately 20 times higher than the permeability in the transverse direction, and, hence, the construction is easily able to remedy the moisture field disturbance incurred by the hole. The electrode distance is approximately 30 mm—this distance is, however, of vanishing importance to the measured MC (Forsén and Tarvainen 2000). Standard power cables were used to connect electrodes and a central terminal box. Banana plugs connected to the external socket of the meter provided the interface between moisture meter and terminal box. This latter interface is a standard interface for many meters with external hammer electrodes.

In all instances but a few, measuring is performed on a weekly basis on Friday morning between 8:00 and 9:00 a.m. For the reported measuring period, two different moisture meters were used—during the first year, a meter with two significant digits and, in the second year, an apparatus with three significant digits were used. Both moisture meters were among the ones tested in Forsén and Tarvainen (2000). The setting of the meters was with respect to temperature 20°C (68°F), irrespective of wood temperature. This minimizes faults in the measuring process and, of course, requires post-measuring correction for wood temperature. The species' setting was chosen to be the best offered but is of no major importance, as the meters were calibrated against reference calibration device with six fixed resistances in the range from 10,000 MOhm to 1.8 MOhm, covering the range 10% to 26.3% moisture content by weight for *Picea abies*. The declared maximum deviation of the fixed resistances is ±2%, and the calibration box used is subjected to external calibration on a regular basis. It is stressed that MC readings in excess of 27% tend to be unstable, or at least not necessarily following the calibration curve used. This is so as the resistance for high MC becomes very low in the order 1 MOhm, and the stability of the accuracy of the meters is not to be trusted in these ranges without careful meter-individual calibration—preferably including electrodes. Such refined calibration has not been performed for the meters and electrode used. Forsén and Tarvainen (2000) are even more conservative with respect to apparatus precision at high MC levels and set an upper limit of 24% MC for a 95% confidence interval within ±1.5% moisture content by weight for well-conditioned material.

The species calibration by use of the reference box resistance, R in MOhm, is the Scandinavian standard calibration curve for moisture-dependent resistance in *Picea abies* of Nordic provenience:

$$\ln(R) = 27.18 \cdot \exp(-0.0852 \cdot MC_{Measured, T_W = 20C}) - 2.30 \quad (9)$$

The temperature correction employed is like the standard correction curve used in Scandinavia, given in Equation 10. The correction requires a device setpoint of 20°C (68°F) and wood temperature input in degree Celsius.

$$MC_{Temp.\ Corrected} = \frac{\left(MC_{Measured,\ setpoint\ T_W = 20C} + 0.567 - 0.0260 \cdot (T_W + 2.8) + 0.000051 \cdot (T_W + 2.8)^2\right)}{\left(0.881 \cdot (1.0056)^{(T_W + 2.8)}\right)} \quad (10)$$

Both the species and temperature calibration formula originate in their latest version from Samuelsson (1990) (for an English version, see Samuelsson [1992]) and are confirmed by the testing performed in Forsén and Tarvainen (2000).

Measuring Results

The field-measured values for wood moisture content—calibrated to correct species by Equation 9 and corrected for temperature by Equation 10—are shown in Figure 5.

The temperature adjustment is made by use of wood temperatures generated in the modeling process by use of actual local climatic data. For all practical purposes, the morning wood temperatures used for the reported lower side measuring points are the same as the simultaneous air temperature. The overall shape of the annual MC oscillation follows the anticipated trend—dry in summer, wet in winter. The measured values in excess of 27% MC by weight should not be interpreted directly as the actual MC due to the mentioned instability of the resistance meters for very low resistances. It is, however, striking that even at these high measured values the weekly oscillation pattern is congruent for all four measuring points.

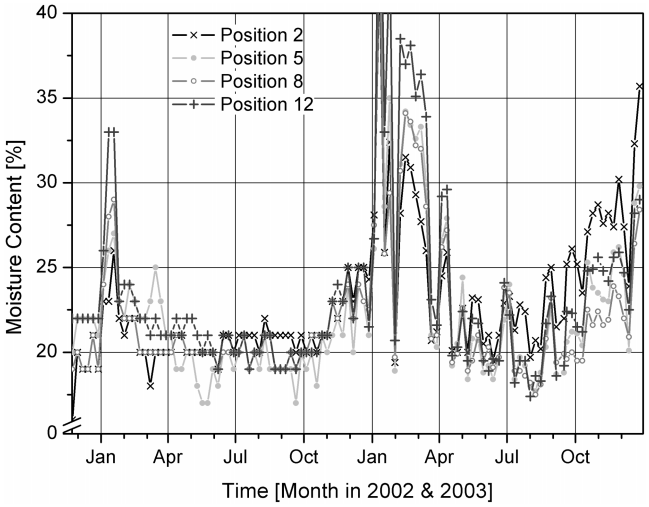

Figure 5 *Experimentally measured MC values at the four instrumented lower positions of the roof of the case study construction (Figure 4); all measured values from the weekly measuring scheme are shown except measurements where values in excess of 40% by weight are truncated by the chosen scale of the diagram.*

From Figure 5 it is observed that the measuring point with the highest winter value (position 12) has the lowest summer readings, whereas the measuring point with the lowest winter value (position 2) has the highest summer value. This indicates that the electrodes in the different points lie in slightly different distances from the exposed lower element surface. This is so as the measuring position closer to the exposed surface will experience larger annual MC amplitude compared to positions closer to the element center where the amplitude is smallest.

MODELING PROCEDURE

General Settings

The roof over the stable was modeled with the computer model presented previously. The model makes hourly calculations of the roof, which is exposed to the outdoor climate. On top of the roof is a black asphalt roof membrane, which is assumed to be vapor tight. The roof has a 22° slope facing west. The computer model makes a detailed calculation of the roof temperature given a solar absorptance of the roof membrane of 0.93 and a longwave emissivity of 0.90. The convective heat transfer coefficient was calculated as a function of the outdoor wind speed. The underside of the roof was exposed to the same air temperature and humidity as that of the outside air, i.e., it was assumed that the livestock did not affect the climate in the open stable. The heat transfer coefficient of the lower surface of the roof was modeled as a constant 25 W/(m²·K) (4.4 Btu/[h·ft^2·°F]), and the vapor transfer coefficient was 6.3·10-8 kg/(Pa·m^2·s) (1090 perm).

The solid wood of the roof was represented by 35 control volumes of thickness, from 1 to 15 mm (0.04 in. to 0.60 in.). The control volumes were distributed such that they corresponded with the locations of the moisture sensors in the roof. Due to a lack of material data for liquid moisture transport, and because the conditions in the stable roof were mainly in the hygroscopic region, liquid moisture transport was not considered explicitly in this analysis. However, the enhanced water vapor permeability at high relative humidity can be seen as some liquid coupled effects of the water, which is absorbed in the wood, and the enhanced vapor permeability was a part of the analysis.

The calculations were carried out with consideration of latent heat of phase change of moisture, which, even for changes of moisture content in the hygroscopic region, involves some small thermal effects.

Two calculation series were carried out for the roof investigated:

1. The first series was run for the roof exposed to the design reference year for Denmark. The purpose was to test the effect of using the different variations of the sorption model in the transient heat and moisture calculation tool. The results for the last of ten consecutive years with identical exposure were used for analysis, i.e., after quasi-steady conditions were attained. The initial condition was an even distribution of a moisture content of 17.5 weight-%.

   Four variations of sorption models were analyzed in the study:

   - With temperature-dependent sorption curves and hysteresis.
   - With temperature-dependent sorption curves without hysteresis. The average between the adsortion and desorption curves was used.
   - Without temperature-dependent sorption curves but with hysteresis. The sorption curve for 20°C (68°F) was used.
   - Without temperature-dependent sorption curves and without hysteresis.

2. The second series was run with actual weather data for the years 2002-2003 for a weather station 20 km (12 miles) from the position of the case study object. The weather data were provided by the Danish Meteorological Institute and comprised hourly values for outdoor air temperature, dew point, solar radiation, wind speed, and cloud index. The purpose of this series was to compare against measured moisture contents from the actual roof for the same two years and to draw some conclusions on the moisture performance of this kind of solid wood construction. The initial moisture content was 20 weight-% as this was measured by the moisture sensors for the beginning. Only the new sorption model with temperature-dependent sorption curves and hysteresis was used for this calculation.

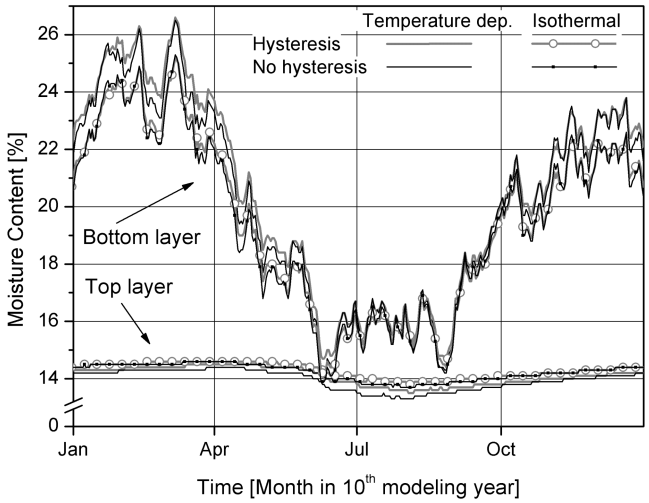

Figure 6 *Moisture content for the last of ten years, calculated with each of the four sorption models. Model results are shown for both a bottom and a top layer of the roof.*

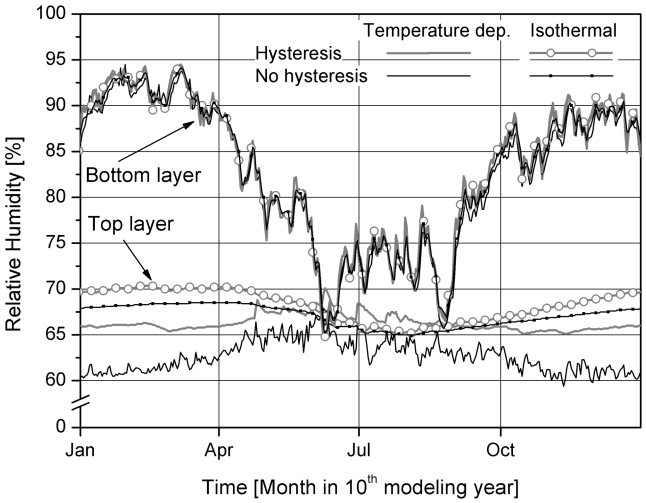

Figure 7 *Relative humidity for the last of ten years, calculated with each of the four sorption models. Model results are shown for both a bottom and a top layer of the roof.*

MODELING RESULTS AND DISCUSSION

Analysis of Sorption Models

Results are presented for the moisture content, relative humidity, and trajectories followed in the sorption diagram—both the conventional two-dimensional sorption diagram (RH-MC) and in the three-dimensional sorption space (T-RH-MC). The calculations have been carried out with hourly time steps. However, in order to avoid the scatter of hourly variations, the results are presented in Figures 6 and 7 as daily mean values.

Figure 6 shows the moisture content during the tenth year of calculation for the top 25 mm (1 in.) of the roof just below the asphalt roof membrane and for the bottom 10 mm (0.4 in.) exposed to the exterior climate. The moisture contents in the top are the dashed lines, which are relatively constant around 14 weight-% moisture. That the moisture content does not vary much can be explained by the tight asphalt roofing felt that comes directly over this part of the wood and the rather large thickness (around 100 mm, 4 in.) of wood that separates this layer from the open surface below. The result is more or less the same for all four sorption models, albeit with a small tendency that the results for the models with temperature-dependent sorption have slightly lower values.

The moisture contents in the bottom of the roof are shown with the solid lines. They show substantial seasonal variation, which is quite natural, as the climate is drier in summer and the open bottom of the roof allows moisture to escape in summer while it is easily adsorbed in winter. In this case, the moisture content tends to be higher by almost 2 weight-% in winter when the temperature-dependent sorption model is used. In either case, there seems to be only a small influence when hysteresis is considered, and then the results with the hysteresis model tend to have the highest moisture contents.

Generally, the moisture content in the top of the roof is drier than in the bottom. A probable reason is the solar heating of the top of the roof, which would cause a lower relative humidity and thereby a lower moisture content in the warm top part of the roof.

Though the maximum values of moisture content exhibit substantial variation with sorption model employed, the effect on the mean moisture content throughout the whole cross section is less pronounced. In broad terms, the effect of including temperature-dependent sorption is a 10% increase of the annual amplitude of the moisture content fluctuation when compared with the models assuming isothermal sorption. Likewise, the effect of including hysteresis in the models reduces the annual amplitude in mean moisture content by 10%.

Figure 7 shows the development of the relative humidity over the tenth year for the same layers. Now it is the relative humidity for the bottom layer (solid lines) that comes out with results that are almost independent of which sorption model is used. A natural explanation is the close connection of this layer with the air below the roof, and the condition of the air seems to dominate the RH level in the wood next to it.

The relative humidity in the top (dashed lines) is first of all lower than in the bottom for most of the year. But the results are quite dependent on which sorption model is used for the calculations. Results with the temperature-dependent sorption

model are lower than the results from using the 20°C (68°F) sorption isotherm. And the results calculated with the hysteresis model are higher than those for the model that uses an average sorption curve between adsorption and desorption. Differences are up to 10% RH and largest in winter.

Recognizing that the relative humidity in the top layer is primarily governed by the moisture content of the wood, as the layer is encapsulated between the vapor-tight asphalt membrane and the 100 mm (4 in.) solid wood below, a heuristic interpretation of the observations can be made along the following lines. The top layer MC by weight increases in the order of 1% from summer to winter, practically irrespective of sorption model (Figure 6). The relative humidity for the two isothermal sorption models is close during the summer. However, the model with hysteresis generates higher wood relative humidity than the model without hysteresis during winter. This is a direct consequence of the modeling assumption: an equal change in moisture content in either of the two models $\Delta MC_{No\ Hys} = \Delta MC_{Hys}$ corresponds to different changes in relative humidity $\Delta RH_{No\ Hys} < \Delta RH_{Hys}$. The same simple interpretation cannot be made between the two temperature-dependent sorption models. However, in a comparison between the temperature-dependent models and the isothermal models, it is obvious that the increase in MC during winter is overridden by the increase in moisture capacity for low temperatures for the temperature-dependent models. Thus, an almost constant relative humidity is seen for the temperature-dependent model with hysteresis, and a decrease in wood relative humidity from summer to winter is seen in the temperature-dependent model without hysteresis.

A sensitivity analysis was carried out to investigate the importance of the moisture content in the wood of the surface coefficients for heat and vapor transfer beneath the roof. The values were still kept constant but either at twice or half the values mentioned in the section, "Modeling Procedure, General Settings." The effect was a change in moisture content of around 0.2% by weight for the wood layers near the bottom surface, while it was hardly noticeable for the layers below the roof membrane. Thus, the convective heat and mass transfer coefficients have only minor importance on the moisture condition of the wood.

Likewise, it was attempted to see the result of neglecting the solar and longwave radiation exchanges at the top surface. Without solar gain, the moisture content of the wood just below the roof membrane increased by about 10% by weight, while the effect was very small for the layers near the lower surface (around 0.25% by weight). If the longwave sky radiation was also cut off (still with no solar radiation), the roof surface experienced no undercooling compared to the ambient, and this resulted in an increase in moisture content by about 8% by weight just below the roof membrane compared to the situation with both solar gain and longwave radiation. So clearly the overheating by the sun and undercooling by sky radiation has an effect on the moisture buildup or removal below the roof membrane.

With knowledge of the daily average values of relative humidity and moisture content, it is possible to plot the (RH, MC)-values as trajectories in the sorption diagram as they develop over the tenth year of calculation. It is mostly interesting to plot such a trajectory for a layer that has some significant variation over time of its RH and MC-values—this will be a layer in the bottom of the roof. The results of the calculation without hysteresis and temperature dependency of the sorption curve yields a trajectory that follows the sorption curve quite exactly. Figures 8 and 9 show the trajectories in the sorption diagram for the respective cases, where either hyster-

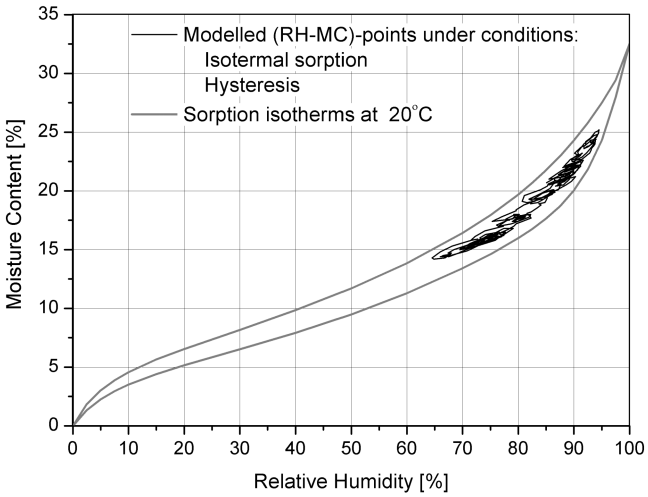

Figure 8 *Trajectory of the (RH-MC) points plotted in the sorption diagram. Case without temperature dependency of the sorption curve but with hysteresis.*

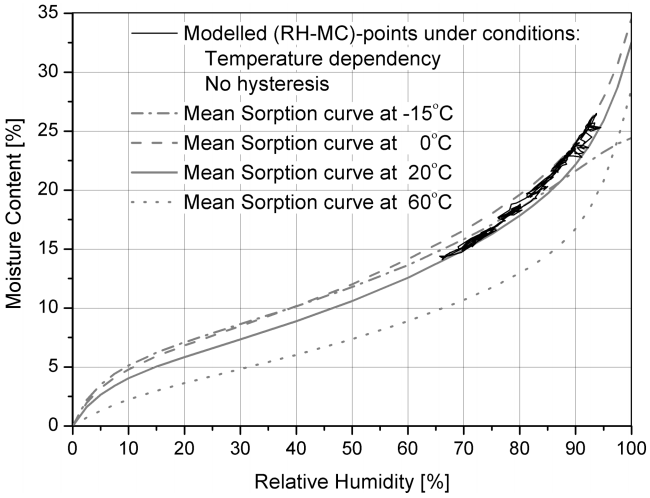

Figure 9 *Trajectory of the (RH-MC) points plotted in the sorption diagram. Case with temperature dependency of the sorption curve but without hysteresis.*

esis or temperature dependency of the sorption curve have been taken into account in the model.

Figure 8 has been drawn with indication of the adsorption and desorption isotherms for 20°C (68°F), and one sees how the calculated values follow scanning curves between the boundaries defined by the adsorption and desorption curves. It may be noted that after each turn of the scanning curve, it sets out with a lower slope than the adsorption and desorption curves from which it originates. This would result in larger RH-variations for given MC-variations when the scanning curves are followed compared to a situation without hysteresis. Thus, hysteresis may seem to result in a lower apparent moisture capacity of the material.

Figure 9 has been drawn with indication of the mean sorption curves at some different temperatures between –15° (5°F) and 60°C (140°F), and one sees how the calculated values mainly lie in the interval between the 0°C (32°F) and 20°C (68°F) isotherms. For relative humidity around 70% RH, the calculated results follow the 20°C sorption isotherm rather closely, whereas, for relative humidity around 90%, the calculated results come closer to the 0°C sorption isotherm. At high relative humidity, e.g., >90% RH, there are some excursions to higher relative humidity even though there is almost no increase in moisture content.

The obvious explanation for these patterns is that the lowest humidity occurs in summer when the temperature is relatively high and, therefore, the condition lies close to the 20°C isotherm. The humidity is highest in winter, when the condition is close to the 0°C isotherm. On days with freezing, the sorption curve lies lower than the 0°C isotherm, and for that reason alone, the relative humidity will increase (excursion toward a higher RH) even when the moisture content does not change much. The temperature in the Danish winter is rather close to the freezing point for most of the time, but typically with a small number of days with freezing down to around –10°C (14°F), and this can explain the excursions.

For temperatures above freezing, the temperature effect on the sorption curve could seem to cause a higher apparent moisture capacity of the materials. Since warming up will typically coincide with drying, and since warming up also means moving toward a lower sorption curve, the combined effect will be a steeper movement in the sorption diagram. Thus, relatively smaller RH-changes will be seen for a given MC-change if it coincides with a temperature change that causes the moisture content to change.

Finally, Figure 10 shows the trajectory of the (T-RH-MC) results (daily averages) in a three-dimensional space diagram when the model for both temperature-dependent sorption and hysteresis is employed. This diagram represents the ultimate combination of the effects discussed above and is meant to give a spatial understanding of the phenomena.

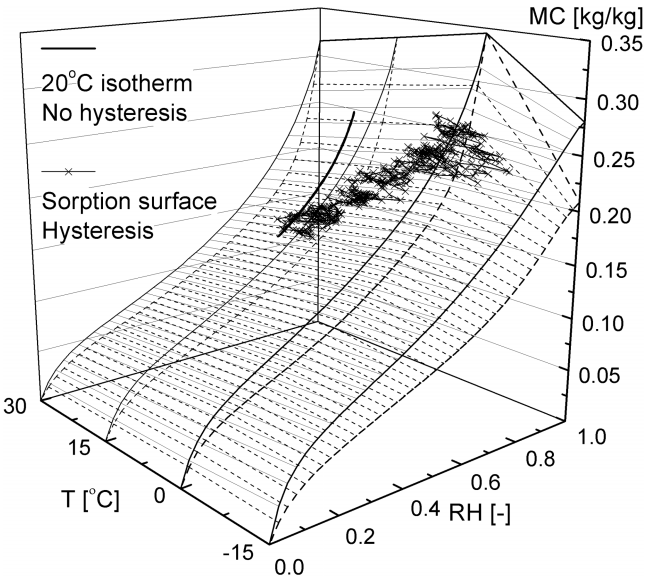

Figure 10 *Trajectory of the (T-RH-MC) points plotted in the sorption space. Case with temperature dependency and hysteresis of the sorption curve. For comparison, the case with an isothermal sorption curve in the 20°C (68°F) plane calculated without hysteresis is also shown.*

Analysis of Field Study

Measured MC values for two of the four measuring positions are shown in comparative plots along with modeled MC values (Figures 11 and 12). The figures truncate the data at MC 27% by weight, tacitly assuming that the measured values above this level are highly doubtful. The fundamental observation made from Figures 11 and 12 is that the modeling catches the weekly oscillations in measured MC to a high degree. This confirms the sensitivity of the weekly measured data to a degree where they cannot be rejected as merely random variation about a grand seasonal variation. The data are even more convincing when recognizing that the climatic data used for modeling are weather data collected approximately 20 km (12 miles) from the site and, thus, does not reflect very local variations arising for instance as function of the livestock below the roof.

Not too much stress should be placed on the apparent ability of the modeling to predict the correct level about which the observed oscillations take place. This is so, as the measurements have accuracy in the order ±1.5% moisture content by weight. Furthermore—and this is the shortcoming of the modeling results presented—the layers used to represent the modeled MC variations are much closer to the lower exposed surface than the nominal positions of the measuring points.

The nominal position of the measuring points implies that they ideally convey the maximum moisture content in a distance between 10 and 35 mm (0.4-1.4 in.) from the exposed

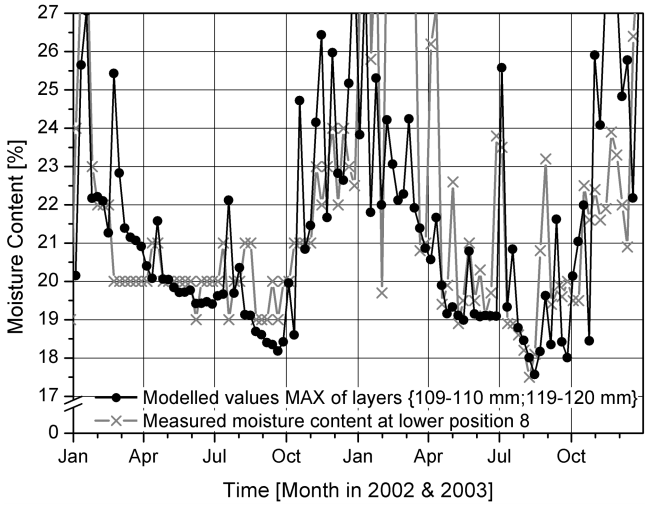

Figure 11 *Measuring results for moisture content at position 8 plotted along with modeled values given as maximum value generated in the outmost layer and a control layer 10 mm inward from the exposed surface.*

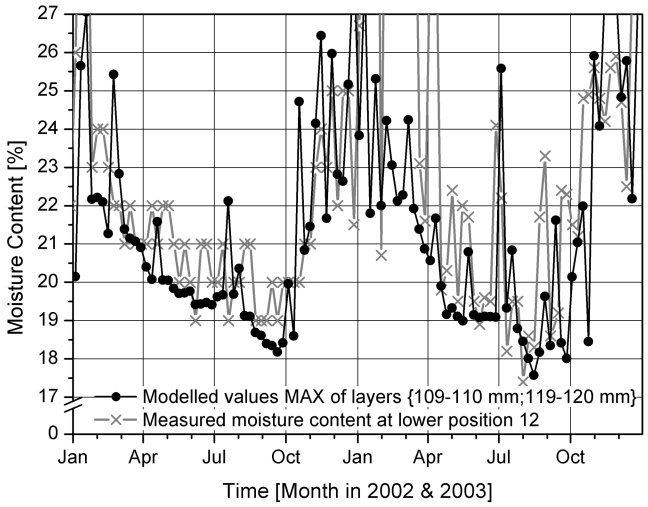

Figure 12 *Measuring results for moisture content at position 12 plotted along with modeled values given as maximum value generated in the outmost layer and a control layer 10 mm inward from the exposed surface.*

surface. However, if the modeled values in the nominal measuring depths are plotted, they cannot catch the rapidness of the measured fluctuations, and the summer moisture content is generally too high. The modeled results shown in Figures 11 and 12 are taken from the bottom 1 mm (0.04 in.) layer and a 1 mm (0.04 in.) layer positioned 10 mm (0.4 in.) behind the exposed surface. Thus, in order to make the modeled and measured values coincide—especially with respect to short-term fluctuation—it has been necessary to assume:

- The measured values convey MC closer to the exposed surface than the nominal measuring depths.
- The measured values convey MC over a shorter depth than the length of the electrodes.

In other words, it seems that the modeling results exhibit too small penetration depth for the moisture content fluctuation. This observation lends itself to the conclusion that the modeling makes use of too-low transport coefficients, restricting the maximum variations to a more surface close region.

Insofar as the modeling confirms that what is being measured is not just random error but actual encountered MC variations in the construction, the shortcoming of the modeling with regard to penetration depth of these variations can relatively easily be remedied by changes to the permeability function, δ_p(RH). The data sets behind the permeability function (Figure 3) leave plenty of room for such a shift of the permeability function toward higher values.

CONCLUSION

The paper presents the development and use of a model that takes the temperature effect of sorption into account in the modeling of moisture transport of wood. The model is implemented as an extension to an existing computer model based on an implicit finite control volume method formulated with the vapor pressure as driving potential.

For implementation in the computer model, adsorption and desorption surfaces in (T-RH-MC)-space for *Picea abies* (Norway spruce) have been constructed in accordance with general thermodynamic considerations and the available experimental data from the literature.

The surface has been established with hindsight to model the moisture content development in a case study construction, where thick wood elements in the roofing on one side are freely exposed to the ambient climate. The moisture content has been surveyed over a period of two years and the measured data are compared to modeled values, the latter generated by use of climatic data covering the site of the construction.

With respect to the fundamental principles of the modeling, the applied variations to the sorption model have been made, covering all four combinations of a sorption model, respectively, with or without hysteresis and with or without temperature dependency. The conclusions for this part of the study are:

- Including hysteresis results in a lower apparent moisture capacity of the material, i.e., a given increment of relative humidity gives a smaller increment of moisture content when a model including hysteresis between

adsorption and desorption is compared to a model using a mean value of the adsorption and desorption branches to express the sorption characteristic.

- For temperatures above freezing, the temperature effect on the sorption curve causes a higher apparent moisture capacity of the material, i.e., a given increment of relative humidity gives a larger increment of moisture content when a model including temperature-dependent sorption is compared to a model using an isothermal sorption characteristic. This observation is to a high degree governed by the fact that periods with high values of ambient relative humidity coincide with periods with low ambient temperatures, where temperature-dependent equilibrium moisture content has the highest values. Correspondingly, low values of ambient relative humidity are met in periods with high ambient temperature, where the equilibrium moisture content is lower.

When applying the new modeling principle in a specific case—the solid wood construction used as an example in this paper—the effect on the yearly amplitude of the mean moisture content is as follows: the amplitude of moisture content becomes 10% smaller when including hysteresis in the modeling; the amplitude of moisture content becomes 10% larger when including temperature dependency in the modeling. However, for cases with other climate histories, and especially in the case of smaller dimensions in the direction of the moisture gradient, these reported effects might be larger.

With respect to the comparison of how the measured and modeled moisture content develop in the case study construction, the following two conclusions are drawn:

- The modeling strongly supports that the measured fluctuations of moisture content are real moisture fluctuations encountered in the construction as a fair degree of congruence between modeled and measured values is observed.
- The modeled values exhibit a smaller penetration depth for short-term moisture content fluctuations than the measured values. This deviation of the modeling may be explained by the water vapor permeability values used and can be proposed remedied by increasing the values of the water vapor permeability function. Such a change to this empirically established function can easily be justified by the available data.

ACKNOWLEDGMENTS

The establishment of a sorption surface was made possible through a literature study financed by the Danish Research Councils through the research project, "Modelling the effects of moisture and load history on the mechanical properties of wood" (grant no. 991363). The same project has financed the analysis of the measured data for the purpose of this paper. C. O. Clorius, when employed at the Danish Technological Institute, Wood Technology, undertook the field-measuring project as part of a Nordic Industrial Fund project for enhancing the documentation for solid wood building elements. The Institute is thanked for making the results available for academic research, and special thanks are given to stable master Christian Vingaard Christensen at the Centre for Living Cultural Heritage at the Danish Agricultural Museum, Gammel Estrup, for volunteering and meticulously carrying on weekly measuring of moisture content in the roof of the instrumented stable construction.

REFERENCES

Ahlgren, L. 1972. Moisture fixation in porous building materials. Division of Building Technology, Lund Institute of Technology, Report 36.Lund, Sweden.

Andersen, A. Helbo, and C. Rode. 2002. MATCH—Moisture and Temperature Calculations for Constructions of Hygroscopical Materials. (www.match-box.dk). Bygge- og Miljøteknik A/S, Vedbæk, Denmark, Ed. 2002 V. 1.6.

Arfvidsson, J. 1999. A new algorithm to calculate the isothermal moisture penetration for periodically varying relative humidity at the boundary. *Nordic Journal of Building Physics*, Vol 2.

Bingye, H., and S. Avramidis. 2003. Wood sorption fractality in the hygroscopic range. Part II, New Model Development and Validation. *Wood and Fiber Science* 35(4):601-608.

Clorius, C.O., and J. Ljørring. 2003. Fluctuations of moisture content in glued solid wood elements at outdoor covered climate conditions. Danish Technological Institute, Wood Technology. (http://solidwood.teknologisk.dk/).

Clorius, C.O., and M.U. Pedersen. 2003. Long-term moisture equilibrium for wood in nordic climates – A catalogue for picea abies exposed to the climatological standard normal at 15 positions. Technical University of Denmark, Technical Report BYG*DTU SR-03-15.

Clorius, C.O. 2003. Modelling moisture induced deformations in glulam structure. *Proceedings of 16th Nordic Seminar on Computational Mechanics. Trondheim, Norway.*

Cudinov, B.S., M.D. Andreev, V.I. Stephanov, and A.V. Finkel'štejn. 1978a. Die Hygroskopizität des Holzes bei Temperaturen under 0ºC, Teil 1: Sorption und Faserstättigungspunkt. Holztechnologie 19(1):91-94.

Cudinov, B.S., M.D. Andreev, V.I. Stephanov, and A.V. Finkel'štejn. 1978b. Die Hygroskopizität des Holzes bei Temperaturen under 0ºC, Teil 2: Der Zustand der hygroskopichen Feuchtigkeit und die Gleichgewichtsfeuchte. Holztechnologie 19(3):174-151.

Drewes, H. 1985. Ausgleichsfeucten von Holzwerkstoffen für das Bauwesen. Holz als Roh- und Werkstoff 43:97-103.

Eurocode 5. 2001. DS/ENV 1995-1-1, Design of timber structures—Part 1.1: General rules and rules for buildings.

Forest Products Society. 1999. Wood Handbook, Wood as an Engineering material. ISBN 1-892529-02-5. USA.

Forsén, H., and V. Tarvainen. 2000. Accuracy and functionality of hand held wood moisture content meters. Technical Research Centre of Finland. VTT Publications 420. Finland.

Goossens, E. 2003. Moisture transfer properties of coated gypsum, Doctoral thesis. Faculty of Architecture, Building and Planning. Eindhoven University of Technology, The Netherlands.

Fynholm, P., and C. Clorius. 2002. Water vapour permeability of solid wood elements, Danish Technological Institute, Wood Technology—Træteknik.

Hansen, K.K. 1986. Sorption Isoterms—A catalogue. Technical University of Denmark, Department of Civil Engineering, Building Materials Laboratory. Technical report 162/86.

Hedenblad, G. 1996. Materialedata för fukttransportberäkninger. Byggforskningsrådet, Fuktsäkerhet i byggnader, T19:1996. Stockholm, Sweden. (in Swedish).

Hedlin, C.P. 1967. Sorption isotherms of twelve woods at subfreezing temperatures. *Forest Products Journal* 17(12):43-48.

Håkansson, H. 1998. Retarded sorption in wood, Ph.D.-dissertation. Lund University—Sweden, Department of Building Science. Report TABK-98/1012.

Karagiozis, A.N. 2001. Impact of air leakage on the thermal and moisture performance of the building envelope. Air Barriers III: Air Barriers Solutions for Buildings in North American Climates, Conference. Washington D.C.

Kelsey, K.E. 1956. The sorption of water vapour by wood. *Australian Journal of Applied Science* 8(1):42-54.

Kollmann, F.F.P., and W.A. Côté. 1968. Principles of Wood Science and Technology. Part I, Solid Wood. Springer-Verlag.

Krabbenhøft, K. 2003. Moisture transport in wood—A study of Physical-Mathematical Models and their Numerical Implementation, Ph.D.-dissertation. Technical University of Denmark, Department of Civil Engineering.

Nielsen, L.F. 1989. Moisture sorption in porous materials—A rational fit procedure. Festschrift Rupert.

Springenschmid: Baustoffe-Forschung, Anwendung, Bewärung, pp. 293-299. Baustoff Institut, Techniche Universität München of Civil Engineering.

Pedersen, C. Rode. 1990a. Combined heat and moisture transfer in building constructions, Ph.D. thesis. Thermal Insulation Laboratory, Technical University of Denmark.

Pedersen, C. Rode. 1990b. Transient calculations of moisture migration using a simplified description of hysteresis in the sorption isotherm. *Proceedings of the 2nd symposion on Building Physics in the Nordic Countries. Technical University of Norway, Trondheim, Norway.*

Peuhkuri, R. 2003. Moisture dynamics in building envelopes, Ph.D. thesis. Department of Civil Engineering, Technical University of Denmark.

Samuelsson, A. 1990. Resistanskurvor för elektriska fuktvortsmätare. (In Swedish) Swedish Institute for Wood Technology Research, Report L 9006029.

Samuelsson, A. 1992. Calibration curves for resistance-type moisture meters. *Proceedings of 3rd IUFRO International Wood Drying Conference, Vienna*, pp. 405-408.

Sellevold, E.J., F. Radjy, P. Hoffmeyer, and L. Bach. 1975. Low temperature internal friction and dynamic modulus for beech wood. *Wood and Fiber* 7(3):162-169.

Skaar, C. 1988. Wood-water relations. Springer-Verlag.

Stamm, A.J., and W. K. Loughborough. 1935. Thermodynamics of swelling of wood. *J Phys Chem* 39:121-132.

Stamm, A.J. 1964. *Wood and Cellulose Science*. The Ronald Press Company.

Strømdahl, K. 2000. Water sorption in wood and plant fibres, Ph.D.-dissertation, Technical University of Denmark, Department of Civil Engineering, Series R-78.

Tveit, A. 1966. Measurements of moisture sorption and moisture permeability of porous materials. Norwegian Building Research Institute, Rapport 45. NBI, Oslo.

Venkateswaran, A. 1970. Sorption of aqueous and nonaqueous media by wood and cellulose. *Chenical Reviews* 70(6):619-637.

Wadsö, L. 1993. Studies of water vapour transport and sorption in wood, Doctoral Dissertation, Report TVBM-1013. Building Materials, Lund University.